Science Advances
AAAS

Supplementary Materials for

Hypertrophic cardiomyopathy–associated mutations drive stromal activation via EGFR-mediated paracrine signaling

Jourdan K. Ewoldt *et al.*

Corresponding author: Christopher S. Chen, chencs@bu.edu

Sci. Adv. **10**, eadi6927 (2024)
DOI: 10.1126/sciadv.adi6927

This PDF file includes:

Figs. S1 to S14

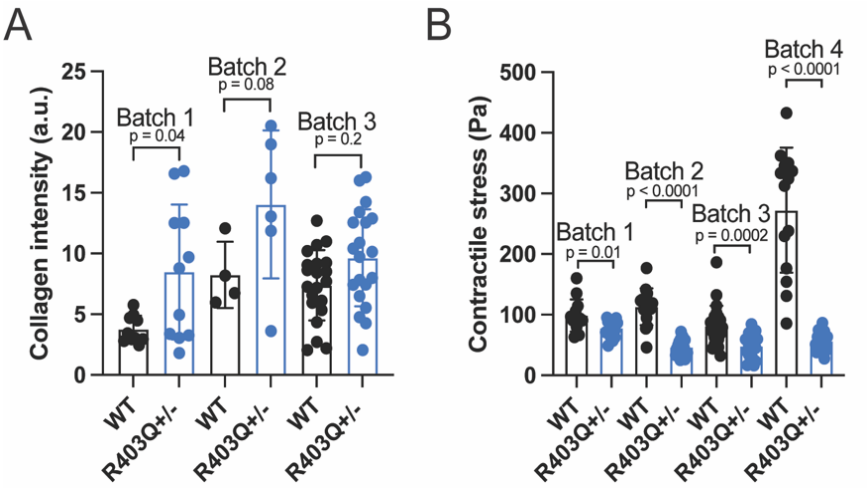

Fig. S1. Batch-to-batch variability in R403Q+/- CMT experiments. (**A**) Collagen intensity of WT and R403Q+/- CMTs from Fig. 1C broken down by mean and standard deviation each of the three batches (n = 4-21 for each group). (**B**) Contractile stress of WT and R403Q+/- CMTs from Fig. 1G broken down by mean and standard deviation each of the four batches (n = 13-23 for each group). Data were assessed with a two-tailed, non-parametric t-test.

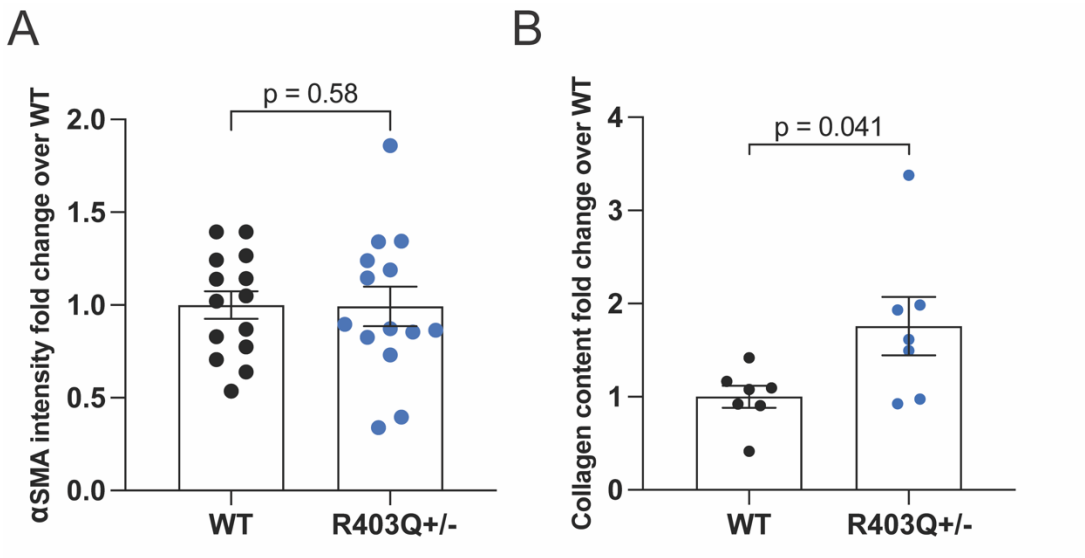

Fig. S2. Characterization of R403Q+/- CMT stromal activation. (**A**) Quantification of the average intensity of alpha-smooth muscle actin (αSMA) in R403Q+/- normalized to WT (n = 14) to minimize noise emerging from batch-to-batch variability (N = 2). Individual CMTs (n) across all independent experiments (N) are shown with means ± SEM. (**B**) Hydroxyproline assay of WT and R403Q+/- CMTs (n = 7 samples) (N = 3). Individual run samples (n), containing 3 pooled CMTs each, across all independent experiments (N) are shown with means ± standard error of the mean (SEM).

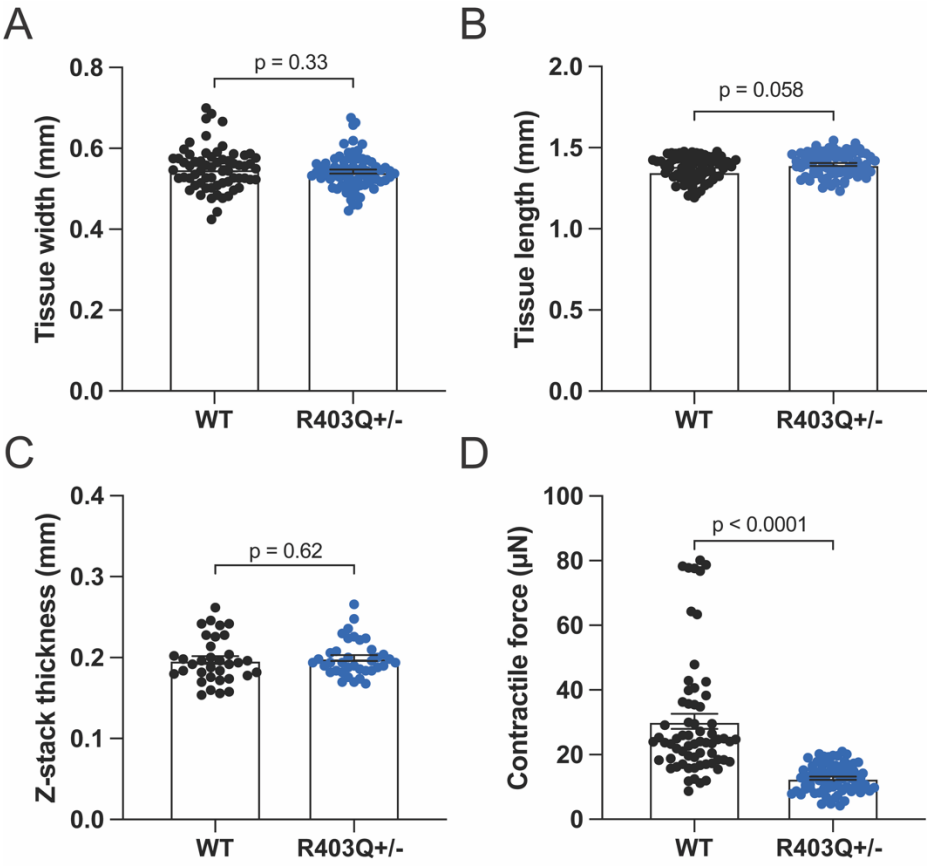

Fig. S3. Dimensions and contractile force of R403Q+/- CMTs. The (**A**) width and (**B**) length of CMTs: WT (n = 65), R403Q+/- (n = 73) (N = 4). (**C**) Thickness of the z-stacks used to quantify collagen deposition in CMTs: WT (n = 34), R403Q+/- (n = 37) (N = 3). Individual CMTs (n) across all independent experiments (N) are shown with means ± SEM. (**D**) Contractile forces of CMTs: WT (n = 64), R403Q+/- (n = 73) (N = 4). Individual CMTs (n) across all independent experiments (N) are shown with means ± SEM.

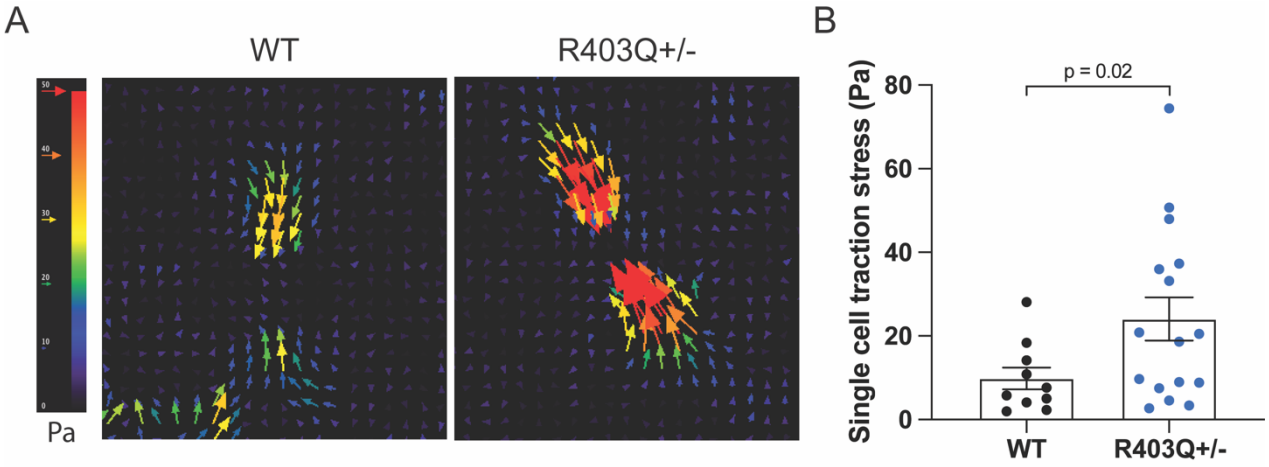

Fig. S4. Single-cell traction force microscopy of R403Q+/- hiPSC-CMs on 7.9 kPa polyacrylamide gels. (**A**) Representative traction force maps of single WT (left) and R403Q+/- (right) hiPSC-CMs on 7.9 kPa polyacrylamide gel substrates. (**B**) Contractile stress of hiPSC-CMs, quantified from single-cell traction force microscopy: WT (n = 10), R403Q+/- (n = 16) (N = 2). Individual hiPSC-CMs (n) across all independent experiments (N) are shown with means ± SEM.

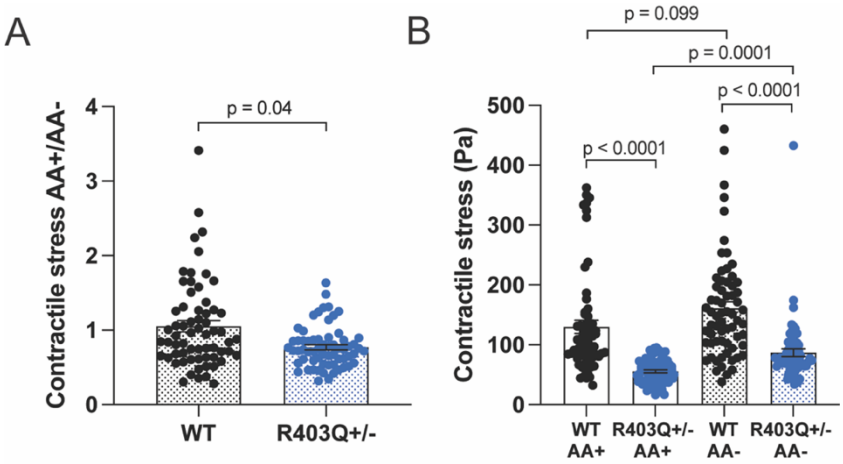

Fig. S5. Effect of ascorbic acid on WT and R403Q+/- CMTs. (**A**) The ratio of the contractile stress of CMTs with ascorbic acid (AA+) compared to CMTs with ascorbic acid removed from culture (AA-): WT (n = 61), R403Q+/- (n = 71) (N = 4). (**B**) Contractile stress of CMTs with and without ascorbic acid (AA): WT with AA (n = 61), R403Q+/- with AA (N = 71), WT without AA (n = 65), R403Q+/- without AA (n = 64) (N = 4). Individual CMTs (n) across all independent experiments (N) are shown with means ± SEM.

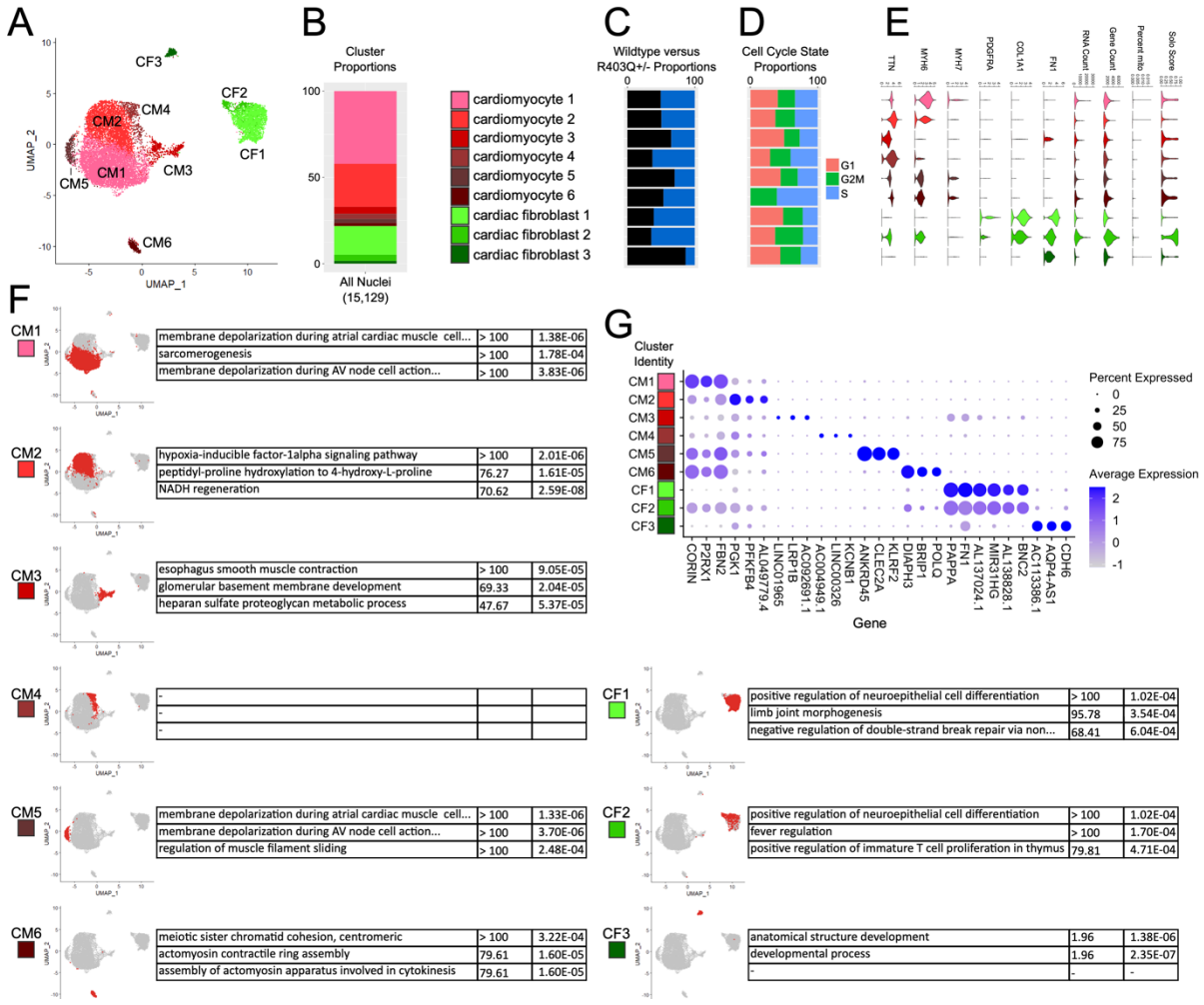

Fig. S6. Cluster specific analysis of gene expression in CMTs (**A**) UMAP of snRNA-sequencing of CMTs separated by cell type. (**B**) Stacked bar plot of cellular abundance in CMTs with cell identity legend. (**C**) Proportion of cells attributed to either WT (black, left) or R403Q+/- (blue, right) CMTs. (**D**) Cell cycle composition of each cluster. (**E**) Canonical markers used to identify cell type in each cluster of (A). (**F**) Quality control metrics of single-cell data. (**G**) Dot plot of unbiased top 3 marker genes for each cluster, compared to each other subcluster.

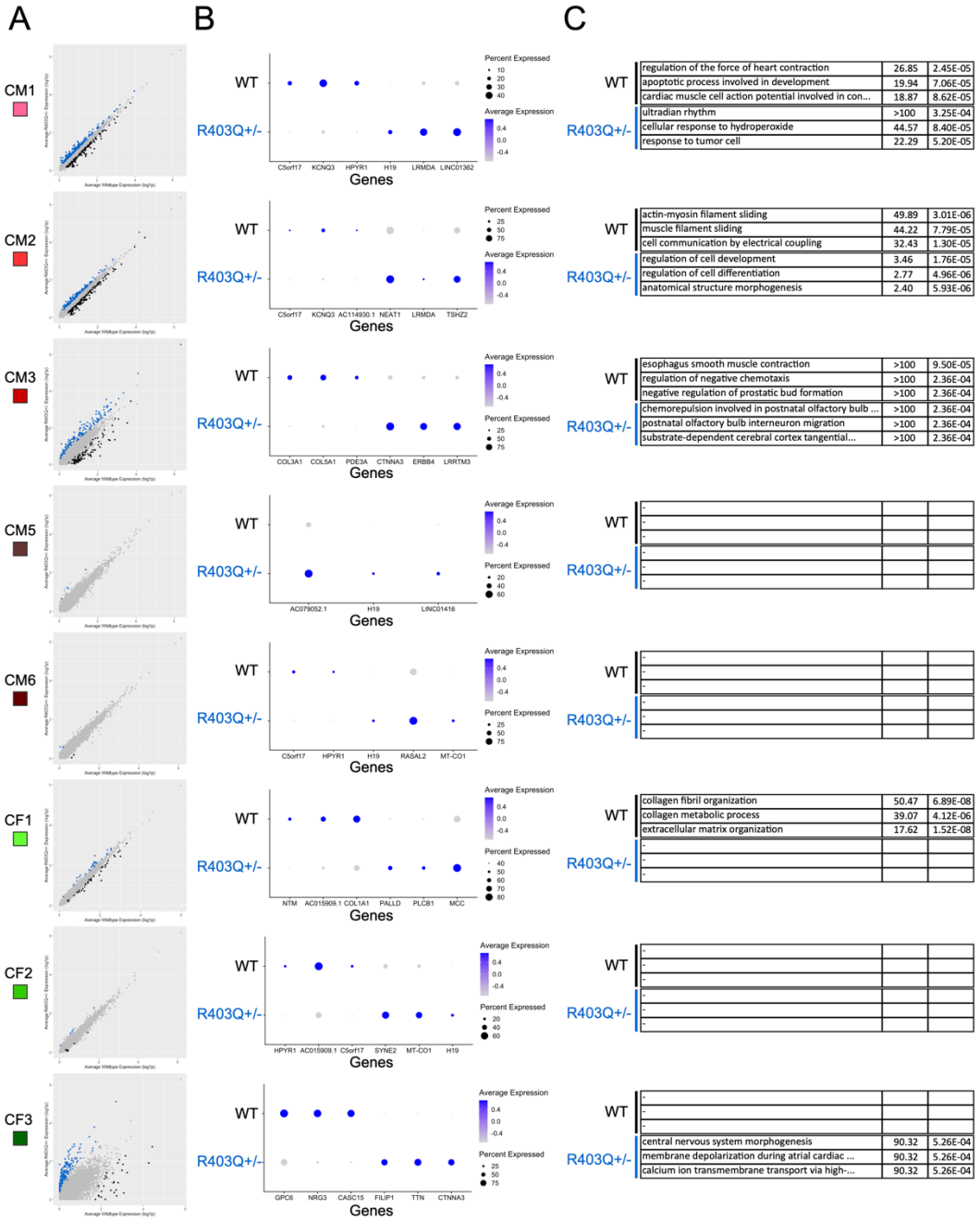

Fig. S7. Cluster specific analysis of differential gene expression between WT and R403Q+/- CMTs. (A) Average gene expression of WT compared to R403Q+/- CMTs, black indicates upregulated in WT, blue indicates upregulated in R403Q+/-. (B) Dot plots for the top 3 genes upregulated in each condition for each cluster. (**C**) Top 3 gene ontology terms for each condition for each subcluster, black bars indicate GO terms for WT and blue bars indicate GO terms for R403Q+/-, ordered by fold-enrichment, with p-value listed on right. CM5, CM6, and CF2 have no GO terms upregulated.

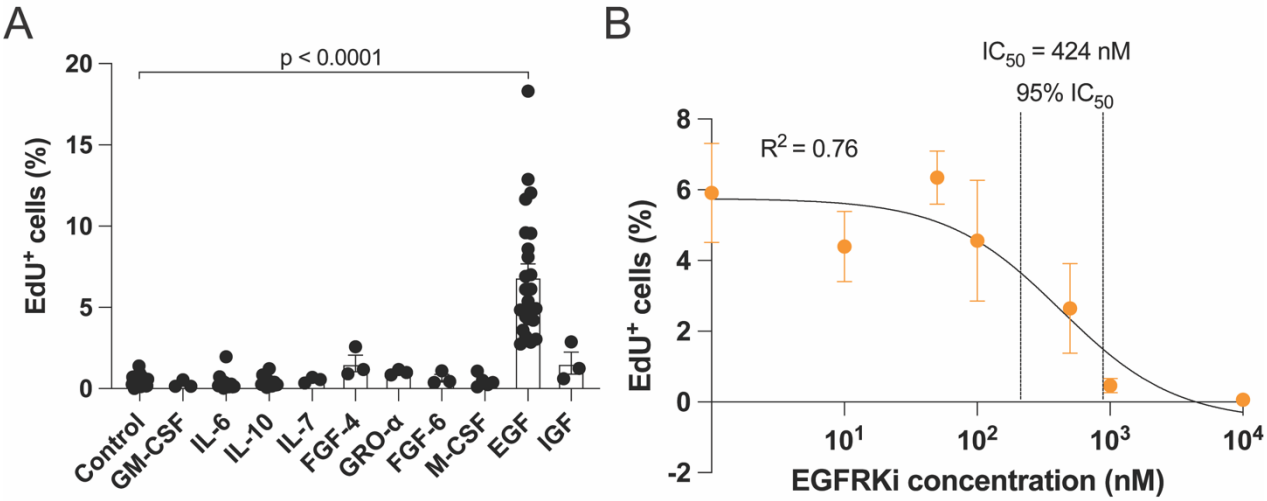

Fig. S8. Effect of paracrine factor signaling on vCF proliferation. (**A**) Average percentage of EdU^+ vCFs after incubation with EdU during hours 20-24 of culture in 10 ng/mL of ten different human recombinant proteins (n > 3, N >=1). (**B**) Average percentage of EdU^+ vCFs after incubation with EdU during hours 20-24 of culture in 100 ng/mL of rhEGF and varying concentrations of EGFRKi. A non-linear fit curve shows that the IC_{50} of EGFRKi is 424 nM and that there was a minimal proliferative response to rhEGF at 1 *μM (n = 3)*. Individual sample wells (n) across all independent experiments (N) are shown with means ± SEM for (A) and means ± standard deviation for (B).

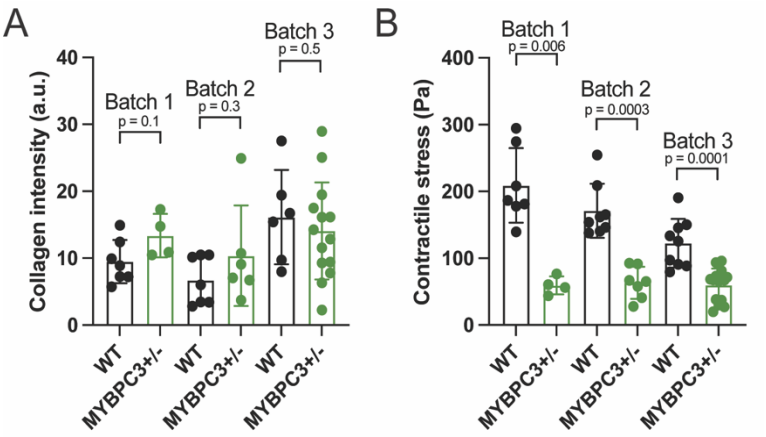

Fig. S9. Batch-to-batch variability in MYBPC3t/+ CMT experiments. (**A**) Collagen intensity of WT and MYBPC3t/+ CMTs from Fig. 5A broken down by mean and standard deviation each of the three batches (n = 4-14 for each group). (**B**) Contractile stress of WT and MYBPC3t/+ CMTs from Fig. 5D broken down by mean and standard deviation each of the three batches (n = 4-14 for each group). Data were assessed with a two-tailed, non-parametric t-test.

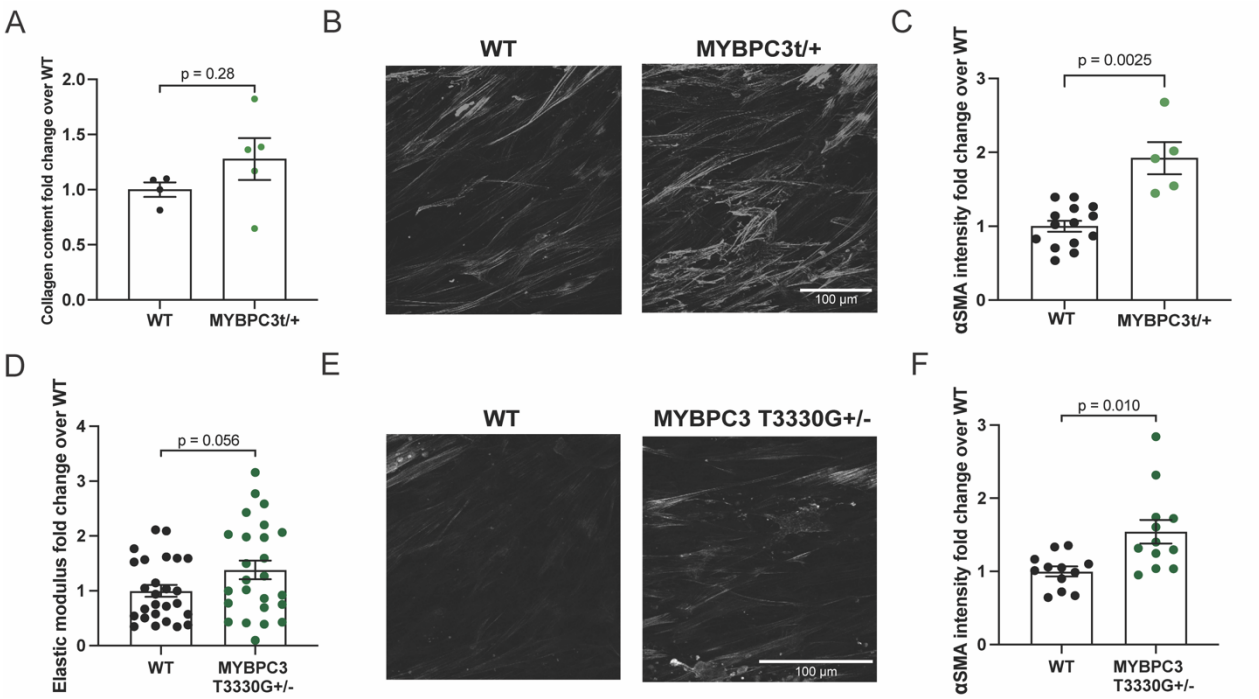

Fig. S10. Further characterization of *MYBPC3*-variant CMTs. (**A**) Hydroxyproline assay of WT (n = 4 samples) and MYBPC3t/+ CMTs (n = 5 samples) (N = 2). Individual run samples (n), containing 3 pooled CMTs each, across all independent experiments (N) are shown with means ± standard error of the mean (SEM). (**B**) Representative images of maximum intensity z-projections of CMTs fixed and stained for alpha-smooth muscle actin (αSMA) on day 7. Scale bar, 100 µm. (**C**) Quantification of average intensity of αSMA in MYBPC3t/+ (n = 5) CMTs normalized to WT (n = 7) (N = 1). Data were assessed with a two-tailed, non-parametric t-test in (A) and (C). (**D**) Elastic moduli of CMTs normalized to WT CMTs: WT (n = 26), MYBPC3 T3330G+/- (n = 25) (N = 4). (**E**) Representative images of maximum intensity z-projections of CMTs fixed and stained for αSMA on day 7. Scale bar, 100 µm. (**F**) Quantification of average intensity of αSMA in CMTs normalized to WT: WT (n = 12), MYBPC3 T3330G+/- (n = 12) (N=3). Individual CMTs (n) across all independent experiments (N) are shown with means ± SEM.

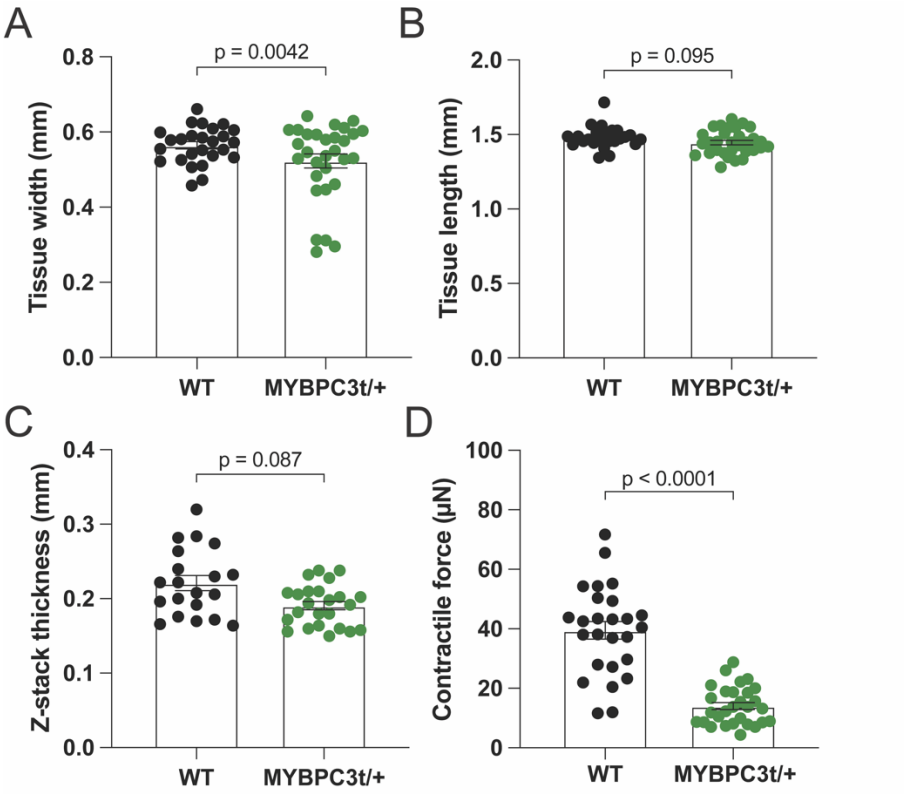

Fig. S11. Dimensions and contractile force of MYBPC3t/+ CMTs. The (**A**) width and **(B**) length of CMTs: WT (n = 31), MYBPC3t/+ (n = 25) (N = 3). (**C**) The thickness of the z-stacks used to quantify collagen deposition between WT (n = 20) and MYBPC3t/+ CMTs (n = 24) (N = 3). (**D**) Contractile forces of CMTs: WT (n = 26), MYBPC3t/+ (n = 29) (N = 3). Individual CMTs (n) across all independent experiments (N) are shown with means ± SEM.

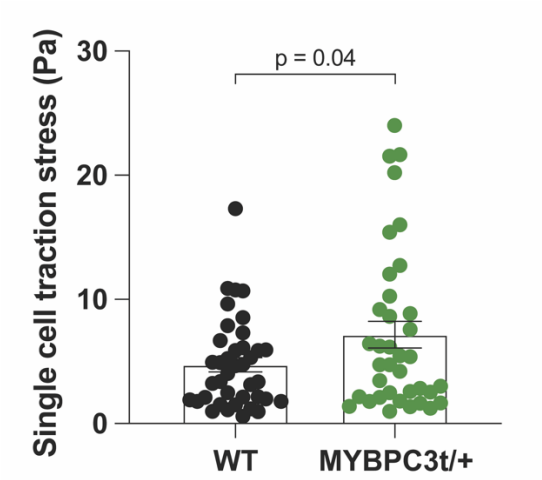

Fig. S12. Single-cell traction force microscopy of MYBPC3t/+ hiPSC-CMs on 7.9 kPa polyacrylamide gels. Contractile stress of hiPSC-CMs, quantified from single-cell traction force microscopy: WT (n = 39), MYBPC3t/+ (n = 37) (N = 2). Individual hiPSC-CMs (n) across all independent experiments (N) are shown with means ± SEM.

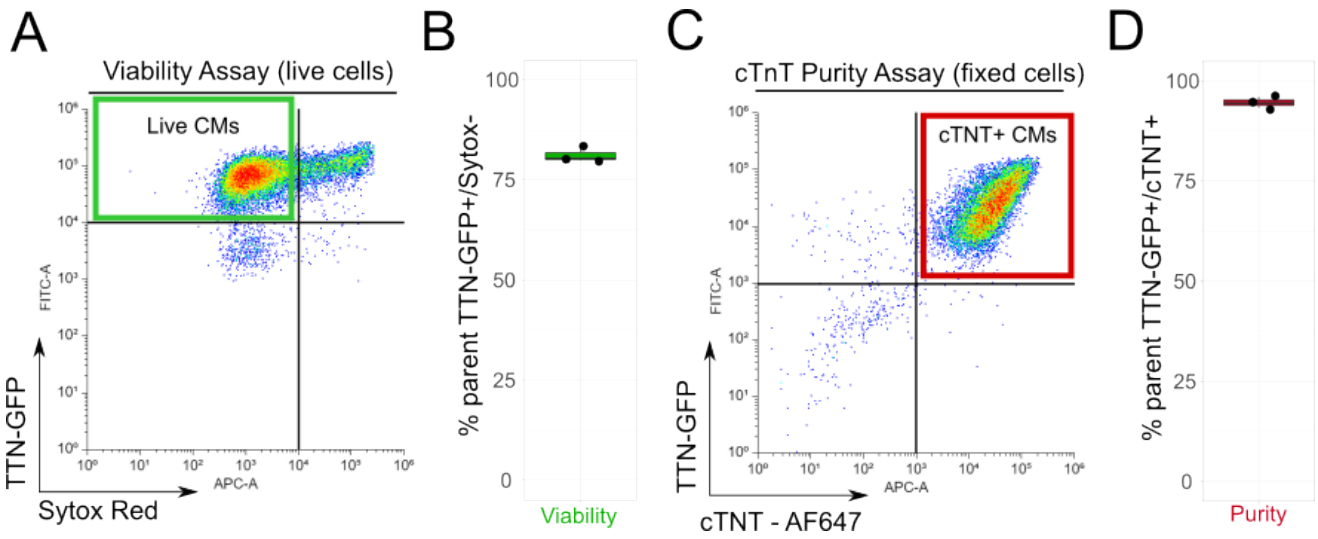

Fig. S13. Viability and purity of cryopreserved cells. Representative flow cytometry analysis of cryopreserved hiPSC-CMs after 2-7 days in culture. (**A**) Live cells were gated as TTN-GFP+/Sytox. (**B**) The average viability of hiPSC-CMs across N = 3 batches. (**C**) Cardiomyocytes were gated as positive for cardiac troponin T (CTnT), TTN-GFP+/cTNT+. (**D**) The average purity of cTnT+ cells in hiPSC-CMs across N = 3 batches.

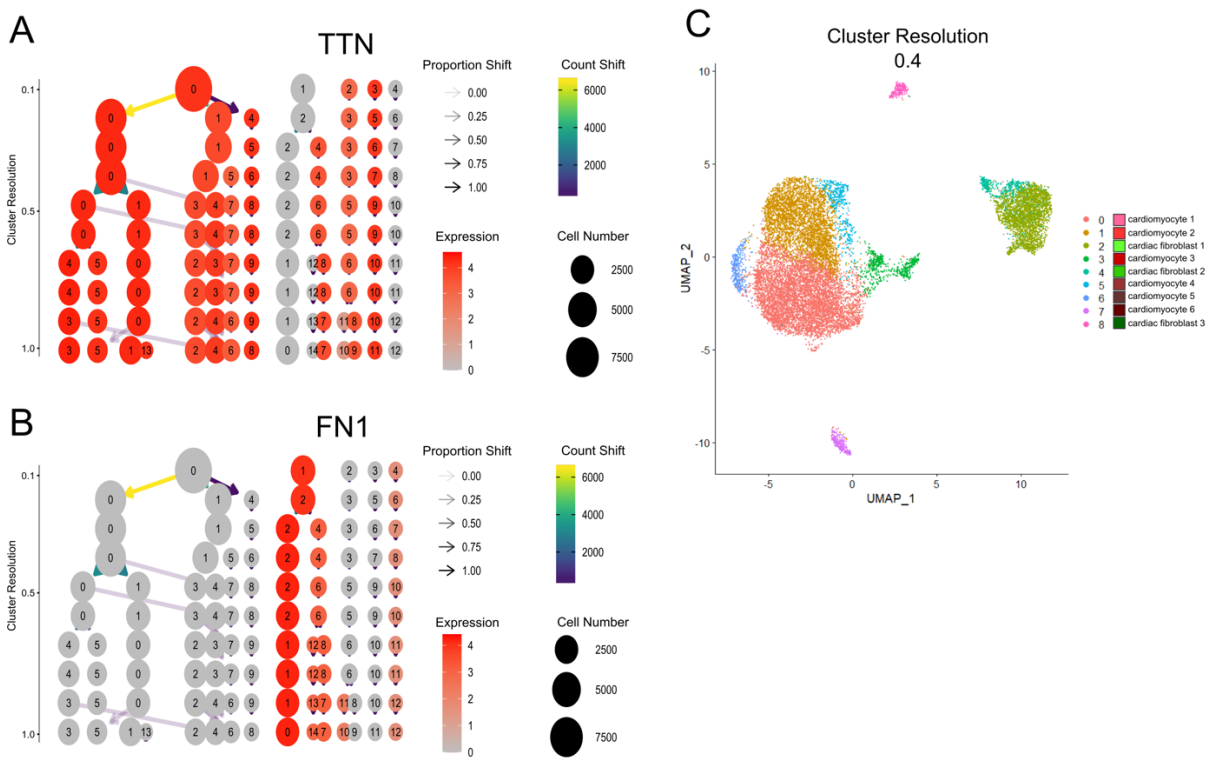

Fig. S14. Hierarchical cluster identity evolution to determine functional cell types. Hierarchical cluster evolution showing median (**A**) *TTN* and (**B**) *FN1* expression across all cells within each cluster. (**C**) UMAP of all cells at a resolution of 0.4, indicating the unbiased cluster assignment with the corresponding cell identity annotations.